Power losses in the screens of the flat single-pole high-current busduct

Tomasz Szczegielniak, Zygmunt Piątek, Dariusz Kusiak
Czestochowa University of Technology
42-200 Częstochowa, ul. Brzeźnicka 60a, e-mail: szczegielniakt@interia.pl

This paper presents an analytical method for determining the power losses in the screens of the three-phase gas-insulated transmission line (i.e., high-current busduct) of circular cross-section geometry. The mathematical model takes into account the skin effect and the proximity effects, as well as the complete electromagnetic coupling between phase conductors and enclosures (i.e., screens). The power losses produced by high-current busducts are usually calculated numerically with the use of a computer. However, the analytical calculation of the power losses is preferable, because it results in a mathematical expression for showing its dependences on various parameters of the line arrangement. Moreover, knowledge of the relations between electrodynamics and constructional parameters is necessary in the optimization construction process of the high-current busducts.

KEYWORDS: analytical method, high-current busduct, electromagnetic field, power losses

1. Introduction

Following the development of thermal and hydroelectric power stations, at the beginning of the 30s, high-current transmission lines (gas-insulated lines GILs) with screened busducts connecting big generators with unit transformers began to be installed. Due to the necessity of transmitting power becoming higher and higher, and to the environmental protection requirements, the length of the line was to be a few kilometers [1-8]. It is estimated that until now the length of the existing lines of that type has not surpassed 100 km. GILs used for high power transmission have been described several times, e.g. in Refs. [1-8]. The gas most often used for insulation is SF_6 (sulphur hexafluoride) whose pressure values range from 0.29 to 0.51 MPa (at 20°C). Recently, SF_6 has been replaced with the 95% mixture of nitrogen N_2 and 5% of SF_6 of 1.3 MPa pressure, or with a 90% mixture of nitrogen N_2 and 10% of SF_6 of 0.94 MPa pressure, as well as with a 80% mixture of nitrogen N_2 and 20% of SF_6 of 0.71 MPa pressure corresponding to the 0.4 MPa pressure in the case when pure SF_6 is used. The contemporary solutions consist of transmission lines insulated with air at atmospheric pressure, with duty-rated voltage values reaching up to 36 kV and duty-rated current values reaching up to: 10 kA for hydroelectric power plants, 20 kA for thermal and nuclear plants whose duty-rated power values reach up to 900 MW, 31.5 kA for nuclear plants with power value of 1300 MW [1-7].

Fig. 1. Flat three-phase high-current busduct [5]

Today high-current busducts are applied in many projects around the world when high-power transmission with high reliability and maximum availability is required. The size of the projects are constantly increasing: from typically some hundred meters system length to typically several kilometers [1-7].

The design of the busducts used for high currents and voltages causes a necessity of precise describing of electromagnetic, dynamic and thermal effects. Knowledge of the relations between electrodynamics and constructional parameters is necessary in the optimization construction process of the high current busducts [1-7].

Power losses depend on value of currents, but for the large cross-sectional dimensions of the phase conductor, even for industrial frequency, skin, external and internal proximity effect should be taken into account [6-8].

2. Electromagnetic field in the screens of the flat three-phase high-current busduct

Let us consider the electromagnetic field in the screens of the flat three-phase high-current busduct presented in the Fig. 2.

In the case of three-phase single-pole high-current busduct shown in Fig. 2 the total current density in the first screen e_1 is a sum of currents induced by each conductor, that is to say

$$\underline{J}_{e1}(r,\Theta)=\underline{J}_{e11}(r,\Theta)+\underline{J}_{e12}(r,\Theta)+\underline{J}_{e13}(r,\Theta)=\underline{J}_{e11}(r,\Theta)+\underline{J}_{e123}(r,\Theta) \tag{1}$$

The total density current in the first screen $\underline{J}_{e1}(r,\Theta)$ depends on currents $\underline{I}_1$, $\underline{I}_2$, $\underline{I}_3$. If these currents form a positive sequence [6-8]

$$\underline{I}_2=\exp[-\mathrm{j}\frac{2}{3}\pi]\,\underline{I}_1 \quad \text{and} \quad \underline{I}_3=\exp[\mathrm{j}\frac{2}{3}\pi]\,\underline{I}_1 \tag{2}$$

then current density $\underline{J}_{e1}(r,\Theta)$ has a form

$$\underline{J}_{e11}(r)=\frac{\underline{\Gamma}_e\,\underline{I}_1}{2\pi\,R_3}\,\underline{j}_{e0}(r)=\frac{\underline{\Gamma}_e\,\underline{I}_1}{2\pi\,R_3}\,\frac{\underline{b}_0\;I_0(\underline{\Gamma}_e\,r)+\underline{c}_0\;K_0(\underline{\Gamma}_e\,r)}{\underline{d}_0} \tag{3}$$

where

$$\underline{d}_0=I_1(\underline{\Gamma}_e R_4)\;K_1(\underline{\Gamma}_e R_3)-I_1(\underline{\Gamma}_e R_3)\;K_1(\underline{\Gamma}_e R_4) \tag{3a}$$

$$\underline{b}_0=\beta_e\;K_1(\underline{\Gamma}_e R_3)-K_1(\underline{\Gamma}_e R_4) \tag{3b}$$

$$\underline{c}_0=\beta_e\;I_1(\underline{\Gamma}_e R_3)-I_1(\underline{\Gamma}_e R_4) \tag{3c}$$

$$\beta_e=\frac{R_3}{R_4}\quad(0\le\beta_e\le 1) \tag{3d}$$

whereas current density $\underline{J}_{e123}(r,\Theta)$ can be expressed as follows

$$\underline{J}_{e123}(r,\Theta)=\underline{J}_{e12}(r,\Theta)+\underline{J}_{e13}(r,\Theta)=-\frac{\underline{\Gamma}_e\,\underline{I}_1}{\pi\,R_4}\sum_{n=1}^{\infty}\underline{A}_n\left(\frac{R_4}{d}\right)^n\underline{f}_{ne}(r)\cos n\Theta \tag{4}$$

where

$$\underline{A}_n=-\frac{1}{2}\left[\left(1+2^{-n}\right)+\mathrm{j}\sqrt{3}\left(1-2^{-n}\right)\right]=A_n\,\exp[\mathrm{j}\,\varphi_n] \tag{4a}$$

$$A_n=\sqrt{1-2^{-n}+4^{-n}} \tag{4b}$$

$$\varphi_n=-\pi+\mathrm{arctg}\frac{\sqrt{3}\left(1-2^{-n}\right)}{1+2^{-n}} \tag{4c}$$

and

$$\underline{f}_{ne}(r)=\frac{K_{n+1}(\underline{\Gamma}_e R_3)\;I_n(\underline{\Gamma}_e r)+I_{n+1}(\underline{\Gamma}_e R_3)\;K_n(\underline{\Gamma}_e r)}{I_{n-1}(\underline{\Gamma}_e R_4)\;K_{n+1}(\underline{\Gamma}_e R_3)-I_{n+1}(\underline{\Gamma}_e R_3)\;K_{n-1}(\underline{\Gamma}_e R_4)} \tag{5}$$

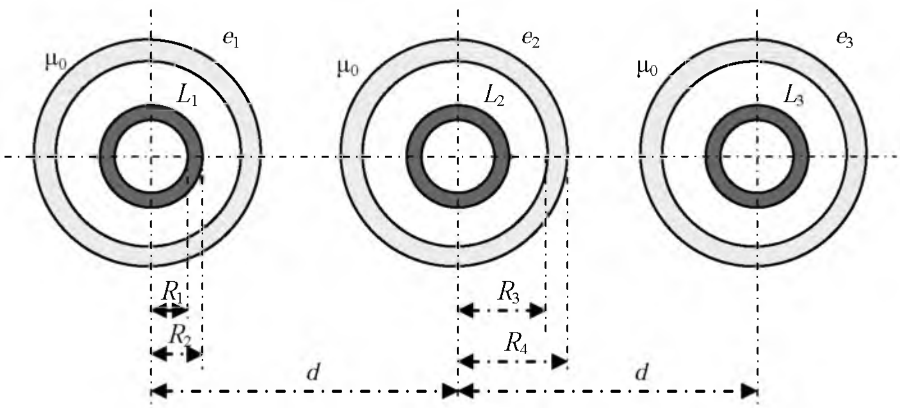

Fig. 2. Flat three-phase high-current busduct

In the above formulas $I_0(\underline{\Gamma}_e r)$, $K_0(\underline{\Gamma}_e r)$, $I_1(\underline{\Gamma}_e r)$, $K_1(\underline{\Gamma}_e r)$, $I_n(\underline{\Gamma}_e r)$, $K_n(\underline{\Gamma}_e r)$, $I_{n-1}(\underline{\Gamma}_e r)$, $K_{n-1}(\underline{\Gamma}_e r)$, $I_{n+1}(\underline{\Gamma}_e r)$ and $K_{n+1}(\underline{\Gamma}_e r)$ are modified Bessel's functions, 0, 1, n, n-1 and n+1 order, calculated for $r = R_3$ and $r = R_4$ [9], and the complex propagation constant of electromagnetic wave in the screen equals

$$\underline{\Gamma}_\mathrm{e} = \sqrt{\mathrm{j}\,\omega\,\mu_0\,\gamma_\mathrm{e}} = \sqrt{\omega\,\mu_0\,\gamma_\mathrm{e}}\,\exp[\mathrm{j}\frac{\pi}{4}] = k_\mathrm{e} + \mathrm{j}\,k_\mathrm{e} \tag{6}$$

with the attenuation constant

$$k = \sqrt{\frac{\omega\mu_0\gamma_e}{2}} = \frac{1}{\delta} \tag{7}$$

where δ is the electrical skin depth of the electromagnetic wave penetration into the conducting environment, ω is an angular frequency, γ_e means conductivity of the screen, and $\mu_0 = 4\pi 10^{-7}\ \mathrm{H\cdot m^{-1}}$ is magnetic permeability of the vacuum.

Total electric field in the first screen has a form

$$\begin{aligned}\underline{E}_{e1}(r,\Theta) &= \underline{E}_{e11}(r) + \underline{E}_{e123}(r,\Theta) = \\ &= \frac{\underline{\Gamma}_\mathrm{e}\,\underline{I}_1}{2\,\pi\gamma_e\,R_3}\left[\underline{j}_{e0}(r) - 2\frac{R_3}{R_4}\sum_{n=1}^{\infty}\underline{A}_n\left(\frac{R_4}{d}\right)^n \underline{f}_{ne}(r)\cos n\Theta\right]\end{aligned} \tag{8}$$

The total magnetic field in the first screen e_1 is defined by formula

$$\underline{\boldsymbol{H}}_{e1}(r,\Theta) = \underline{\boldsymbol{H}}_{e11}(r) + \underline{\boldsymbol{H}}_{e12}(r,\Theta) + \underline{\boldsymbol{H}}_{e13}(r,\Theta) = \mathbf{1}_r\underline{H}_{e1r}(r,\Theta) + \mathbf{1}_\Theta\underline{H}_{e1\Theta}(r,\Theta) \tag{9}$$

in which the radial component takes the following form

$$\underline{H}_{e1r}(r,\Theta) = -\frac{\underline{I}_1}{\pi\,\underline{\Gamma}_\mathrm{e}\,R_4\,r}\sum_{n=1}^{\infty}\underline{A}_n\left(\frac{R_4}{d}\right)^n n\,\underline{f}_{ne}(r)\ \sin n\Theta \tag{10}$$

while the tangent component

$$\begin{aligned}\underline{H}_{e1\Theta}(r,\Theta) &= \frac{\underline{I}_1}{2\,\pi\,R_3}\times \\ &\left\{\underline{h}_{e0}(r) - \frac{2R_3}{\underline{\Gamma}_\mathrm{e}R_4\,r}\sum_{n=1}^{\infty}\underline{A}_n\left(\frac{R_4}{d}\right)^n\left[-n\,\underline{f}_{ne}(r) + \underline{g}_{ne}(r)\right]\cos n\Theta\right\}\end{aligned} \tag{11}$$

where

$$\underline{h}_{e0}(r) = \frac{\underline{I}}{2\,\pi\,R_3}\,\frac{\underline{b}_0\,I_1(\underline{\Gamma}_\mathrm{e}r) - \underline{c}_0\,K_1(\underline{\Gamma}_\mathrm{e}r)}{\underline{d}_0} \tag{11a}$$

and

$$\underline{g}_e(r) = \underline{\Gamma}_\mathrm{e}\,r\,\frac{K_{n+1}(\underline{\Gamma}_\mathrm{e}\,R_3)\,I_{n-1}(\underline{\Gamma}\,r) - I_{n+1}(\underline{\Gamma}_\mathrm{e}\,R_3)\,K_{n-1}(\underline{\Gamma}_\mathrm{e}\,r)}{I_{n-1}(\underline{\Gamma}_\mathrm{e}\,R_4)\,K_{n+1}(\underline{\Gamma}_\mathrm{e}R_3) - I_{n+1}(\underline{\Gamma}_\mathrm{e}\,R_3)\,K_{n-1}(\underline{\Gamma}_\mathrm{e}\,R_4)} \tag{11b}$$

The current density and magnetic field in the second screen e_2 are defined by Eqs. (1) and (9), respectively, in which current $\underline{I}_1$ should be replaced with $\underline{I}_2$ and constant $\underline{A}_n$ with constant

$$\underline{B}_n = \frac{1}{2}\left\{-\left[(-1)^n + 1\right] + \mathrm{j}\sqrt{3}\left[(-1)^n - 1\right]\right\} \tag{12}$$

Formulas for screen e_3 are obtained in the same way by replacing $\underline{I}_1$ and $\underline{A}_n$, respectively, with $\underline{I}_3$ and

$$\underline{C}_n = \frac{(-1)^n}{2}\left[-\left(1 + 2^{-n}\right) + \mathrm{j}\sqrt{3}\left(1 - 2^{-n}\right)\right] \tag{13}$$

3. Power losses in the screens of the flat single-pole high-current busduct

Apparent power of the first screen is equal [7, 8]

$$\underline{S}_{e1} = -\oiint_S \left[\underline{\boldsymbol{E}}_{e1}(r) \times \underline{\boldsymbol{H}}^*_{e1}(r)\right] \cdot \mathrm{d}\boldsymbol{S} = P_{e1} + \mathrm{j}\, Q_{e1} \tag{14}$$

from where

$$\underline{S}_{e1} = \underline{S}_{e0} + \underline{S}_{e123} \tag{15}$$

where

$$\underline{S}_{e0} = \frac{\Gamma_e\, l\, I^2}{2\,\pi\,\gamma_e R_3^2}\left\{R_4\left[\underline{j}_{e0}(R_4)\underline{h}^*_{e0}(R_4)\right] - R_3\left[\underline{j}_{e0}(R_3)\underline{h}^*_{e0}(R_3)\right]\right\} \tag{15a}$$

and

$$\underline{S}_{e123} = \frac{jI^2 l}{\pi\gamma_e R_4^2}\sum_{n=1}^{\infty}\underline{A}_n^2\left(\frac{R_4}{d}\right)^{2n}\left\{\begin{array}{l}\underline{f}_{ne}(R_4)\left[-n\,\underline{f}_{ne}^{\,*}(R_4) + \underline{g}_{ne}^{\,*}(R_4)\right] \\ -\underline{f}_{ne}(R_3)\left[-n\,\underline{f}_{ne}^{\,*}(R_3) + \underline{g}_{ne}^{\,*}(R_3)\right]\end{array}\right\} \tag{15b}$$

Power losses (active power) in the flat single-pole high-current busduct can be determined with Poynting theorem. But if we use Poynting theorem, we can not isolate the real part (as an active power) and the imaginary part (as a reactive power). It is hard on account of the complex propagation constant and complex modified Bessel's functions. Therefore, the active power will be calculated from Joule-Lenz law [10]:

$$P_{e1} = \iiint_V \frac{1}{\gamma_e}\underline{J}_{e1}(r,\Theta)\,\underline{J}^*_{e1}(r,\Theta)\,\mathrm{d}V = \frac{1}{\gamma_e}\int_0^l\int_0^{2\pi}\int_{R_3}^{R_4}\underline{J}_{e1}(r,\Theta)\,\underline{J}^*_{e1}(r,\Theta)\, r\,\mathrm{d}r\,\mathrm{d}\Theta\,\mathrm{d}z \tag{16}$$

From the formula (16) we get

$$P_{e1} = P_{e0} + P_{e123} \tag{17}$$

where

$$P_{\mathrm{e}0} = \frac{\underline{\Gamma}_{\mathrm{e}}^{*}\, l\, I_1^{\;2}}{4\,\pi\,\gamma_{\mathrm{e}}\,\beta_{\mathrm{e}}^{2}\,R_4}\,\frac{\underline{a}_0}{\underline{d}_0\,\underline{d}_0^{*}} \tag{17a}$$

and

$$P_{\mathrm{e}123} = \frac{\underline{\Gamma}_{e}^{\;*}\, l\, I_1^{2}}{2\,\pi\,\gamma\,R_4}\sum_{n=1}^{\infty} A_n^{2}\left(\frac{R_4}{d}\right)^{2n}\frac{\underline{a}_{ne}}{\underline{b}_{ne}\,\underline{b}_{ne}^{*}} \tag{17b}$$

where

$$\begin{aligned}
\underline{a}_0 = \underline{b}_0\,\underline{b}_0^{*} &\left\{\begin{aligned} & I_0^{*}(\underline{\Gamma}_{\mathrm{e}}R_4)I_1(\underline{\Gamma}_{\mathrm{e}}R_4) + \mathrm{j}\,I_0(\underline{\Gamma}_{\mathrm{e}}R_4)I_1^{*}(\underline{\Gamma}_{\mathrm{e}}R_4) - \\ & -\beta_{\mathrm{e}}\left[I_0^{*}(\underline{\Gamma}_{\mathrm{e}}R_3)I_1(\underline{\Gamma}_{\mathrm{e}}R_3) + \mathrm{j}\,I_0(\underline{\Gamma}_{\mathrm{e}}R_3)I_1^{*}(\underline{\Gamma}_{\mathrm{e}}R_3)\right]\end{aligned}\right\} - \\
-\underline{c}_0\,\underline{c}_0^{*} &\left\{\begin{aligned} & K_0^{*}(\underline{\Gamma}_{\mathrm{e}}R_4)K_1(\underline{\Gamma}_{\mathrm{e}}R_4) + \mathrm{j}\,K_0(\underline{\Gamma}_{\mathrm{e}}R_4)K_1^{*}(\underline{\Gamma}_{\mathrm{e}}R_4) - \\ & -\beta_{\mathrm{e}}\left[K_0^{*}(\underline{\Gamma}_{\mathrm{e}}R_3)K_1(\underline{\Gamma}_{\mathrm{e}}R_3) + \mathrm{j}\,K_0(\underline{\Gamma}_{\mathrm{e}}R_3)K_1^{*}(\underline{\Gamma}_{\mathrm{e}}R_3)\right]\end{aligned}\right\} - \\
-\underline{c}_0\,\underline{b}_0^{*} &\left\{\begin{aligned} & I_0^{*}(\underline{\Gamma}_{\mathrm{e}}R_4)K_1(\underline{\Gamma}_{\mathrm{e}}R_4) - \mathrm{j}\,K_0(\underline{\Gamma}_{\mathrm{e}}R_4)I_1^{*}(\underline{\Gamma}_{\mathrm{e}}R_4) - \\ & -\beta_{\mathrm{e}}\left[I_0^{*}(\underline{\Gamma}_{\mathrm{e}}R_3)K_1(\underline{\Gamma}_{\mathrm{e}}R_3) - \mathrm{j}\,K_0(\underline{\Gamma}_{\mathrm{e}}R_3)I_1^{*}(\underline{\Gamma}_{\mathrm{e}}R_3)\right]\end{aligned}\right\} + \\
+\underline{b}_0\,\underline{c}_0^{*} &\left\{\begin{aligned} & I_1(\underline{\Gamma}_{\mathrm{e}}R_4)K_0^{*}(\underline{\Gamma}_{\mathrm{e}}R_4) - \mathrm{j}\,I_0(\underline{\Gamma}_{\mathrm{e}}R_4)K_1^{*}(\underline{\Gamma}_{\mathrm{e}}R_4) - \\ & -\beta_{\mathrm{e}}\left[I_1(\underline{\Gamma}_{\mathrm{e}}R_3)K_0^{*}(\underline{\Gamma}_{\mathrm{e}}R_3) - \mathrm{j}\,I_0(\underline{\Gamma}_{\mathrm{e}}R_3)K_1^{*}(\underline{\Gamma}_{\mathrm{e}}R_3)\right]\end{aligned}\right\}
\end{aligned} \tag{17c}$$

$$\begin{aligned}
\underline{a}_{\mathrm{ne}} = {} & I_{n+1}(\underline{\Gamma}_{\mathrm{e}}R_4)\,K_{n+1}(\underline{\Gamma}_{\mathrm{e}}R_3)\left[I_{n+1}^{*}(\underline{\Gamma}_{\mathrm{e}}R_3)\,K_n^{*}(\underline{\Gamma}_{\mathrm{e}}R_4) + I_n^{*}(\underline{\Gamma}_{\mathrm{e}}R_4)\,K_{n+1}^{*}(\underline{\Gamma}_{\mathrm{e}}R_3)\right] \\
& + \mathrm{j}\,I_n(\underline{\Gamma}_{\mathrm{e}}R_4)\,K_{n+1}(\underline{\Gamma}_{\mathrm{e}}R_3)\left[I_{n+1}^{*}(\underline{\Gamma}_{\mathrm{e}}R_4)\,K_{n+1}^{*}(\underline{\Gamma}_{\mathrm{e}}R_3) - I_{n+1}^{*}(\underline{\Gamma}_{\mathrm{e}}R_3)\,K_{n+1}^{*}(\underline{\Gamma}_{\mathrm{e}}R_4)\right] - \\
& I_{n+1}(\underline{\Gamma}_{\mathrm{e}}R_3)\left\{\begin{aligned} & K_{n+1}^{*}(\underline{\Gamma}_{\mathrm{e}}R_3)\left[I_n^{*}(\underline{\Gamma}_{\mathrm{e}}R_4)\,K_{n+1}(\underline{\Gamma}_{\mathrm{e}}R_4) - \mathrm{j}\,I_{n+1}^{*}(\underline{\Gamma}_{\mathrm{e}}R_4)\,K_n(\underline{\Gamma}_{\mathrm{e}}R_4)\right] \\ & + I_{n+1}^{*}(\underline{\Gamma}_{\mathrm{e}}R_3)\left[K_n^{*}(\underline{\Gamma}_{\mathrm{e}}R_4)\,K_{n+1}(\underline{\Gamma}_{\mathrm{e}}R_4) + \mathrm{j}\,K_{n+1}^{*}(\underline{\Gamma}_{\mathrm{e}}R_4)\,K_n(\underline{\Gamma}_{\mathrm{e}}R_4)\right]\end{aligned}\right\}
\end{aligned} \tag{17d}$$

$$\underline{b}_{ne} = I_{n-1}(\underline{\Gamma}_{\mathrm{e}}R_4)\,K_{n+1}(\underline{\Gamma}_{\mathrm{e}}R_4) - I_{n+1}(\underline{\Gamma}_{\mathrm{e}}R_4)\,K_{n-1}(\underline{\Gamma}_{\mathrm{e}}R_4) \tag{17e}$$

$$\underline{b}_{ne}^{*} = I_{n-1}^{*}(\underline{\Gamma}_{\mathrm{e}}R_4)\,K_{n+1}^{*}(\underline{\Gamma}_{\mathrm{e}}R_3) - I_{n+1}^{*}(\underline{\Gamma}_{\mathrm{e}}R_3)\,K_{n-1}^{*}(\underline{\Gamma}_{\mathrm{e}}R_4) \tag{17f}$$

If we introduce the reference active power [7-8]

$$P_{0\mathrm{ew}} = \frac{l\, I_1^{\;2}}{\pi\,\gamma_{\mathrm{e}}\,(R_4^{2} - R_3^{2})} \tag{18}$$

then the relative active power in the first screen has a form

$$k_{\mathrm{e}1}^{(P)} = \frac{P_{\mathrm{e}0} + P_{\mathrm{e}123}}{P_{0\mathrm{ew}}} \tag{19}$$

Dependence of the coefficient (19) on parameter α_e for different values of the relative walls thickness β_e of the first screen and of relative distance between conductors λ_e is presented in the Fig. 3 (where $\alpha_e = k_e R_4$, $\lambda_e = \dfrac{d}{R_3}$).

a) b)

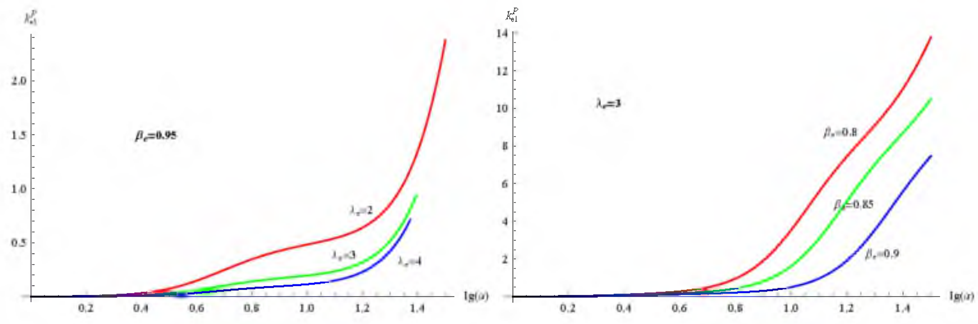

Fig. 3. Dependence of the relative active power in the first screen on parameter α_e:
a) for constant value of the parameter β_e, b) for constant of the parameter λ_e

The reactive power emitted on internal inductance of the first screen, we calculate from (14), thus

$$Q_{e1} = Q_{e0} + Q_{e123} \tag{20}$$

where

$$Q_{e0} = -\mathrm{j}\frac{l\,I^2}{2\pi\gamma_e R_3 \underline{d}_0}\left\{\underline{\Gamma}_e\left[\begin{aligned}&\underline{b}_0\left(I_0(\underline{\Gamma}_e R_4) - I_0(\underline{\Gamma}_e R_3)\right) + \\ &+ \underline{c}_0\left(K_0(\underline{\Gamma}_e R_4) - K_0(\underline{\Gamma}_e R_3)\right)\end{aligned}\right] - \frac{\underline{\Gamma}_e^*\,\underline{a}_0}{2\beta_e\,\underline{d}_0^*}\right\} \tag{20a}$$

and

$$Q_{e123} = \frac{l\,I_1^2}{\pi^2\gamma R_4^2}\sum_{n=1}^{\infty}\left(\int_0^{2\pi} D_n^2\,\mathrm{d}\Theta\right)\left(\frac{R_4}{d}\right)^{2n} \times \left\{\begin{aligned}&n\left[\underline{f}_n(R_3)\,\underline{f}_n^*(R_3) - \underline{f}_n(R_4)\,\underline{f}_n^*(R_4)\right] + \\ &\underline{f}_n(R_4)\,\underline{g}_n^*(R_4) - \underline{f}_n(R_3)\,\underline{g}_n^*(R_3) + \\ &+\mathrm{j}\frac{\underline{\Gamma}_e^*\,R_4}{2}\,\frac{\underline{a}_{ne}}{\underline{b}_{ne}\,\underline{b}_{ne}^*}\end{aligned}\right\} \tag{20b}$$

If we introduce the reference reactive power [7, 8]

$$Q_{0ew} = \mathcal{X}_{0ew}\,I_1^2 = \omega\frac{\mu_0\,l}{2\pi}\left[\frac{R_3^4}{\left(R_4^2 - R_3^2\right)^2}\ln\frac{R_4}{R_3} - \frac{1}{4}\frac{3R_3^2 - R_4^2}{R_4^2 - R_3^2}\right] I_1^2 \tag{21}$$

then the relative reactive power of the first screen has a form

$$k_{\mathrm{e}1}^{(Q)} = \frac{Q_{\mathrm{e}0} + Q_{\mathrm{e}123}}{Q_{0\mathrm{ew}}} \tag{22}$$

Dependence of the coefficient (22) on parameter α_e for different values of the relative walls thickness β_e of the first conductor and of relative distance between conductors λ_e is presented in the Fig. 4.

a) b)

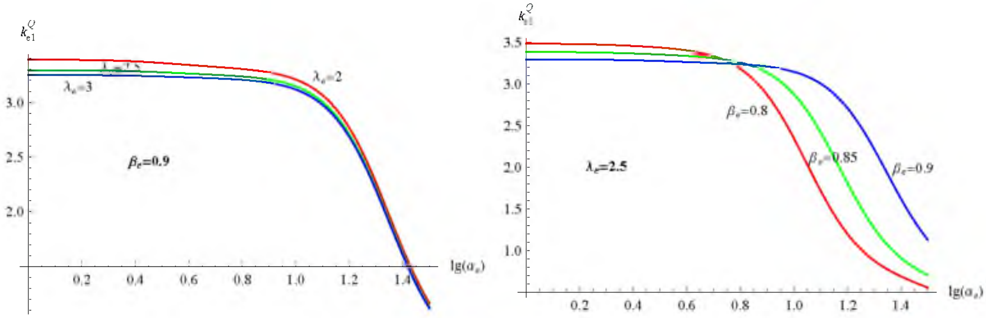

Fig. 4. Dependence of the relative reactive power of the first screen on parameter α_e: a) for constant value of the parameter β_e, b) for constant of the parameter λ_e

In the same way we can calculated power losses in the second and third screen. Besides if we take into account that

$$\int_0^{2\pi} A_n^2 \,\mathrm{d}\Theta = \int_0^{2\pi} C_n^2 \,\mathrm{d}\Theta \tag{23}$$

then

$$k_{e3}^{(P)} = \frac{P_3}{P_{0ew}} = k_{el}^{(P)} \tag{24}$$

and

$$k_{e3}^{(Q)} = \frac{Q_3}{Q_{0ew}} = k_{el}^{(Q)} \tag{25}$$

4. Conclusions

An analytical approach to the solution of the power losses in the screens of the flat single-pole high-current busduct has been presented in this paper. The mathematical model takes into account the skin effect and the proximity effects, as well as the complete electromagnetic coupling between phase conductors and screens.

In produced high-current busducts, for industrial frequency value of parameter α_e is included from 5 to 20. It means that active power in the screens of the flat three-phase high-current busduct can be eight times bigger than the active power calculated without taking into account proximity effect (Fig. 3).

Similarly, reactive power connected with internal inductance of the screen can be three times bigger than the reactive power calculated without taking into account proximity effect (Fig. 4).

Proximity effect depends on geometrical and physical parameters of the flat high-current busduct.

We should add that the total reactive power emitted in the screens of the flat single-pole high-current busduct is a sum of the determined in the paper the reactive power connected with internal inductances of the screens and the reactive power connected with external and mutual inductances of the screens.

References

[1] Nawrowski R.: Tory wielkoprądowe izolowane powietrzem lub SF_6. Wyd. Pol. Poznańskiej, Poznań 1998.
[2] Piątek Z.: Impedances of high-current busducts. WPC, Czestochowa 2008.
[3] CIGRE Brochure No 218.: Gas Insulated Transmission Lines (GIL). WG 23/21/33-15, CIGRE, Paris, 2003.
[4] Koch H.: Gas-Insulated Transmission Line (GIL). John Wiley & Sons, 2012.
[5] Holduct – Z. H. Ltd. Polska.: Szynoprzewody trójfazowe okrągłe. [Online]. Available: http://www.holduct.com.pl/index.php?menu=p2
[6] Kusiak D.: Pole Magnetyczne Dwu i Trójbiegunowych Torów Wielkoprądowych, Praca Doktorska, Częstochowa 2008.
[7] Szczegielniak T.: Straty mocy w nieekranowanych i ekranowanych rurowych torach wielkoprądowych, Praca Doktorska, Gliwice, 2011.
[8] Piątek Z., Szczegielniak T., Kusiak D.: Straty mocy w płaskim rurowym trójfazowym torze wielkoprądowym, Wiadomości Elektrotechniczne, nr 11, s. 9-13, 2009.
[9] Mc Lachlan N.W.: Funkcje Bessela dla inżynierów. PWN, Warszawa 1964.
[10] Krakowski M.: Elektrotechnika teoretyczna. Pole elektromagnetyczne. WN PWN, Warszawa 1995.